Available online at www.sciencedirect.com
SCIENCE DIRECT®
Journal of Power Sources 119–121 (2003) 211–215
JOURNAL OF POWER SOURCES
www.elsevier.com/locate/jpowsour

Emulsion drying preparation of layered $LiMn_xCr_{1-x}O_2$ solid solution and its application to Li-ion battery cathode material

S.-T. Myung[a], S. Komaba[a,*], N. Hirosaki[a], N. Kumagai[a], K. Arai[b], R. Kodama[b], Y. Terada[b], I. Nakai[b]

[a]*Department of Chemical Engineering, Faculty of Engineering, Iwate University, 4-3-5 Ueda, Morioka, Iwate 020-8551, Japan*
[b]*Department of Applied Chemistry, Faculty of Science, Science University of Tokyo, Kagurazaka, Shinjuku, Tokyo 162-8601, Japan*

Abstract

Lithium–chromium–manganese oxides, $LiMn_xCr_{1-x}O_2$ ($0 \le x \le 0.6$), were synthesized as solid solutions by simple calcination of emulsion-dried powder precursor. The product was well crystallized to an α-$NaFeO_2$ structure (space group: $R\bar{3}m$). By combination of Rietveld analysis of X-ray diffraction data and X-ray absorption near edge structure (XANES) techniques, the final product is considered to be $[Li^{I}]^{oct}_{3a}[Mn^{III}_{x}Cr^{III}_{1-x}]^{oct}_{3b}[O_2]_{6c}$ ($0 \le x \le 0.6$). The prepared oxides were electrochemically active, and capacity as cathode materials for lithium-ion battery was improved with increasing Mn substitution amount.

Keywords: $LiMn_xCr_{1-x}O_2$; Lithium; Battery; Rietveld refinement; XANES; Emulsion drying method

1. Introduction

$LiCoO_2$ is one of the best cathode materials for Li-ion batteries with regards to capacity, cycle life and rate capability [1,2]. But the cobalt component is a relatively expensive element and toxic. Another candidate is $LiNiO_2$. This material also shows comparable battery performance as $LiCoO_2$. However, the difficulty of powder preparation due to contamination by Ni^{2+} in the final product and thermal unstability in the over-charged state make it difficult to compete with $LiCoO_2$ [3]. Considering cost, thermal stability, and environmental problems, spinel $LiMn_2O_4$ is a very attractive material for Li-ion battery cathodes material. Even though it shows good rate capability, poor cyclability derived from Mn dissolution in elevated temperature storage is an urgent problem to be solved before adoption as a cathode for Li-ion battery [4]. One more problem is structural degradation by the collective Jahn–Teller distortion on 3 V cycling [5].

Layered types of lithium manganese oxides, such as monoclinic [6,7] and orthorhombic $LiMnO_2$ [8–12], exhibit good battery performance on 3–4 V regions. Even though the original structure of those compounds is gradually transformed by electrochemical cycling to spinel like structure, their unique cycling behaviors in the 3 V region are remarkably interesting because the Jahn–Teller effect due to Mn^{3+} is preferentially predominant, leading to a structural disruption in normal spinel $LiMn_2O_4$ compounds. However, the capacity loss normally associated with this effect is hardly observed in the both monoclinic and orthorhombic $LiMnO_2$ oxides due to the formation of nano-structured domains [13]. The large potential gap between two potential plateaus on 3 and 4 V versus Li may hinder their practical use.

Recently, Li–Mn–Cr–O compounds are intensively being studied as a new candidate of Li-ion battery cathode material [14,15]. Chromium substitution at Mn sites of $Li_2Mn_2O_4$ results in several structural modifications depending on the amount of Cr and calcination temperature. In case of lower level doping, the products are crystallized into tetragonal spinel ($I4_1/amd$) or distorted hexagonal structures ($C2/m$). At higher levels, the structure showed a well-defined trigonal structure ($R\bar{3}m$). In both cases, it is considered that average oxidation states of Mn and Cr are all trivalent, indicating that they can be electrochemically active. Only $Li_2Mn_2O_4$ having hexagonal structure and higher amounts of Cr doping did not transformed to spinel phase during cycling, though the transformation is usually observed in layered $LiMnO_2$. This can be interpreted to mean that the hexagonal structure probably cycles better. Another compound is Li_3MnCrO_5 (solid solution of $LiCrO_2$–Li_2MnO_3) which is the same composition as $Li_{1.2}Mn_{0.4}Cr_{0.4}O_2$ [16,17]. Basically, the

* Corresponding author. Tel.: +81-196216329; fax: +81-196216328.
E-mail address: komaba@iwate-u.ac.jp (S. Komaba).

0378-7753/03/$ – see front matter
doi:10.1016/S0378-7753(03)00181-2

material consists of tetravalent Mn and trivalent Cr, meaning that only Cr can join in electrochemical redox reaction as confirmed by X-ray absorption spectroscopic technique [17].

We recently reported the Li–Mn^{III}–Cr^{III}–O compounds resulting in interesting charge–discharge performance [18]. One of the issues with this compound is how to prepare it, because the solid-solution range of this material was quite narrow [14,15]. Recently, we successfully reported a wide range of solid-solution such as $LiMn_xCr_{1-x}O_2$ ($0 \leq x \leq 0.6$) [18] similar to $LiAl_xMn_{2-x}O_4$ ($0 \leq x \leq 0.6$) [19,20] and $LiNi_{0.5}Mn_{1.5}O_4$ [21] by employing an emulsion drying method which can intermix cations very homogeneously on the atomic scale [22,23]. Here, we report on powder preparation of $LiMn_xCr_{1-x}O_2$ ($0 \leq x \leq 0.6$) and the charge–discharge properties.

2. Experimental

2.1. Powder preparation

The solid solution of $LiMn_xCr_{1-x}O_2$ ($0 \leq x \leq 0.6$) was prepared by the emulsion drying method [22,23] as reported previously [18]. Starting materials used for the synthesis of $LiMn_xCr_{1-x}O_2$ were $LiNO_3$ (Kanto), $Mn(NO_3)_2{\cdot}6H_2O$ (Kanto) and $Cr(NO_3)_3{\cdot}9H_2O$ (Kanto). The emulsion-dried precipitate was burned out for several minutes at 300 °C in air, and then the obtained powders were fired at 400 °C for 6 h in air to oxidize Mn^{II} to Mn^{III} or Mn^{IV}. Subsequently, the powders were calcined at 850 °C for given times in an Ar atmosphere.

2.2. Analysis

To characterize the structure of the prepared materials, X-ray powder diffraction (XRD) measurements were carried out using Cu Kα radiation of a Rigaku Rint 2200 diffractometer. The collected intensity data were analyzed by the Rietveld refinement program, Fullprof 2000 [24]. Transmission electron microscopic (TEM; 200 kV, Hitachi, H-800) observation was carried out to check the products. The Mn and Cr K-edge X-ray absorption near edge structure (XANES) spectra of the as-prepared $LiMn_xCr_{1-x}O_2$ powder were measured in the transmission mode. The measurements were carried out at BL-12C, Photon Factory (PF), KEK, Japan, using a Si(1 1 1) double-crystal monochromator. Manganese and chromium foils were used to calibrate the energy at each edge.

2.3. Battery performance

For electrochemical testing, cathodes were fabricated by blending the prepared powder, acetylene black and polyvinylidene fluoride (80:15:5) in *N*-methylpyrolidinone. The slurry was pasted onto stainless ex-met (1 cm^2). A beaker-type cell consisted of cathode, lithium foil as an anode, and 1 M $LiClO_4$ in ethylene carbonate–dimethyl carbonate (1:1 in volume) as an electrolyte. The assembly of the cells was carried out in an Ar-filled glove box. The cells were first charged, and then discharged between 4.3 and 2.7 V versus Li with a current density of 10 and 20 mA g^{-1} at 25 °C.

3. Results and discussion

3.1. Powder preparation

Fig. 1 shows a Rietveld refinement pattern of $LiMn_{0.6}Cr_{0.4}O_2$ calcined at 850 °C for 12 h in an Ar atmosphere. The space group of $R\bar{3}m$ was chosen as the best structural model. The refinement was done assuming Li atoms in 3*a* sites, Cr and Mn atoms in 3*b* sites, and O atoms in 6*c* sites, as shown in Table 1. The refinement fits the intensities of the Bragg

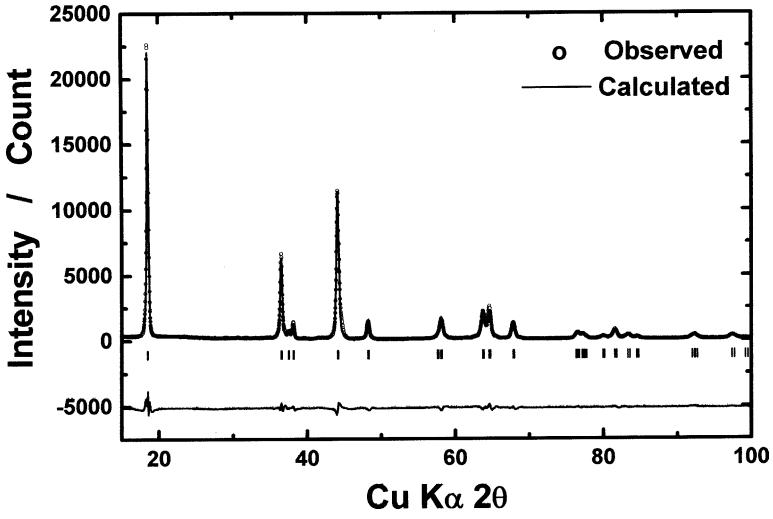

Fig. 1. Rietveld refinement results of powder XRD data for $LiMn_{0.6}Cr_{0.4}O_2$ calcined at 850 °C for 12 h under an Ar atmosphere.

Table 1
Structural parameters obtained from Rietveld refinement of $LiMn_{0.6}Cr_{0.4}O_2$ synthesized by the emulsion drying method

Atom	Site	x	y	z	g
Li	3*a*	0	0	1/2	0.997 (5)
Mn	3*b*	0	0	0	0.597 (4)
Cr	3*b*	0	0	0	0.398 (4)
O	6*c*	0	0	0.2596 (3)	1

Formula: $LiMn_{0.6}Cr_{0.4}O_2$; crystal system: hexagonal; space group: $R\bar{3}m$.

peaks as well as the profile well. This result confirms that $LiMn_{0.6}Cr_{0.4}O_2$ powder has the α-$NaFeO_2$ structure and Mn atoms are doped uniformly at the Cr sites of $LiCrO_2$ ($R\bar{3}m$). Table 2 shows the variation in lattice parameters as a function of the Mn substitution amount. With increasing Mn amount the lattice parameters are getting smaller monotonically, even though the ionic radius of Mn^{3+} (0.645 Å) is larger than that of Cr^{3+} (0.61 Å). Mishra and Ceder [25] have reported the lattice parameters of layered $LiMnO_2$ ($R\bar{3}m$, $a = 2.82$ Å and $c = 14.27$ Å) by simulation optimized with ferromagnetic spin polarization. In the solid solution, once Cr is substituted by Mn, the corresponding lattice parameter should be higher because the ionic radius of Mn^{3+} is higher than that of Cr^{3+}. Comparing with the lattice parameters of $LiCrO_2$ and $LiMnO_2$, however, the lattice parameters of $LiMnO_2$ are relatively smaller than those of $LiCrO_2$. It seems that there is a monotonic variation in the lattice parameters in the solid solution of $LiCrO_2$–$LiMnO_2$. Like this, a linear decrease or increase is usually observed in solid solution compounds. Furthermore, it is well known that when the value of *c*/*a* is larger than 4.9, it can be defined as hexagonal structure ($R\bar{3}m$) [16]. As can be seen in Table 2, the values are more than 4.9, and a high level substitution brings about higher hexagonality. Therefore, the decrease in lattice parameters as a function of Mn doping amount is clear evidence of the solid solution formation, and the range to form single phase is $x \leq 0.6$ in $LiMn_xCr_{1-x}O_2$ [18].

Here, our target material is $LiMn_xCr_{1-x}O_2$ in which Mn is trivalent and Cr is also trivalent. However, it is difficult to measure the oxidation state of the both transition metals by chemical titration method. Because of this difficulty, XANES was used to provide electronic structural information. Fig. 2 shows Mn and Cr K edge XANES spectra of the

Table 2
Variation in lattice parameters of $LiMn_xCr_{1-x}O_2$ powders as a function of Mn amount

x in $LiMn_xCr_{1-x}O_2$	a (Å)	c (Å)	c/a	R_{wp} (%)	R_{Bragg} (%)
0	2.8991	14.4356	4.9792	13.8	4.36
0.25	2.8906	14.4181	4.9879	12.6	3.27
0.5	2.8825	14.3916	4.9926	11.2	2.56
0.6	2.8799	14.3799	4.9931	13.3	3.66

The calculated values were obtained from Rietveld refinement.

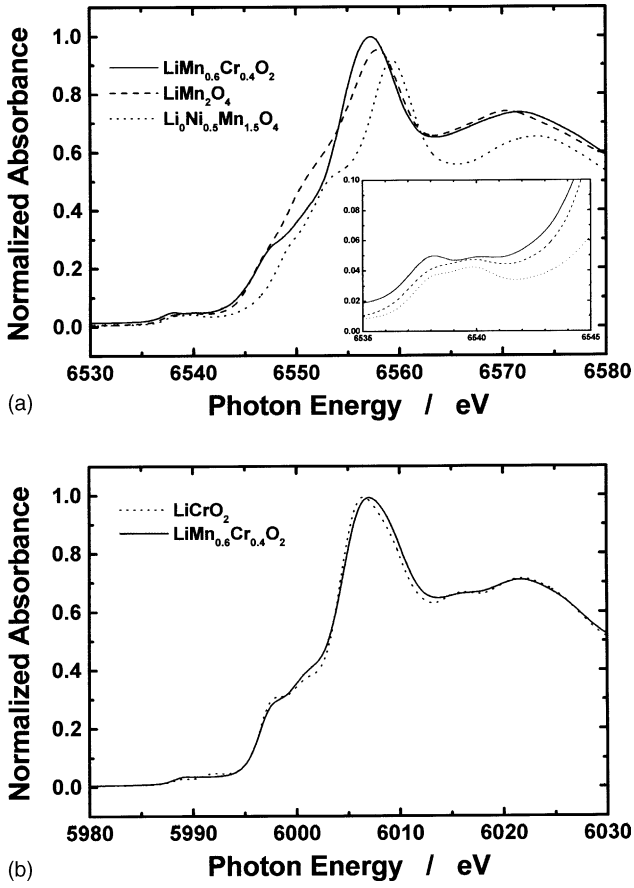

Fig. 2. X-ray absorption near-edge spectra of $LiMn_{0.6}Cr_{0.4}O_2$ calcined at 850 °C for 12 h. (a) Mn K-edge spectrum compared with $LiMn_2O_4$ and $Li_0Ni_{0.5}Mn_{1.5}O_4$; (b) Cr K-edge spectrum compared with $LiCrO_2$.

as-prepared $LiMn_{0.6}Cr_{0.4}O_2$. The manganese spectrum is compared with spinel type of $LiMn_2O_4$ and delithiated $Li_0Ni_{0.5}Mn_{1.5}O_2$. From Fig. 2a, it is clear that the midpoint of absorption edge position (chemical shift) changes in accordance with atomic valence states in compounds, causing an energy shift at the absorption edge [26]. $LiMn_{0.6}Cr_{0.4}O_2$ has the highest pre-edge absorption at 6538 eV while that of the fully delithiated $Li_0Ni_{0.5}Mn_{1.5}O_4$ is located at 6540 eV in Fig. 2a. On the other hand, that of $LiMn_2O_4$ is intermediate between the two or is even close to the latter. From these observations, it can be estimated that Mn in $LiMn_{0.6}Cr_{0.4}O_2$ is in the trivalent state. For the case of chromium in Fig. 2b, the spectrum is practically identical with $LiCrO_2$, indicating the Cr is trivalent and the coordination environments in the two compounds are similar. By combination of the Rietveld analysis of the X-ray diffraction data and XANES examinations, it is assumed that Mn and Cr in $LiMn_{0.6}Cr_{0.4}O_2$ powders is trivalent with octahedral coordination.

Fig. 3 shows TEM bright-field images of $LiMn_{0.5}Cr_{0.5}O_2$ calcined at 850 °C. The observed particles are uniform. The particle distribution greatly depended on the calcination time. For 12 h calcination shown in Fig. 3a, the particle size distribution was quite narrow, and the size is estimated

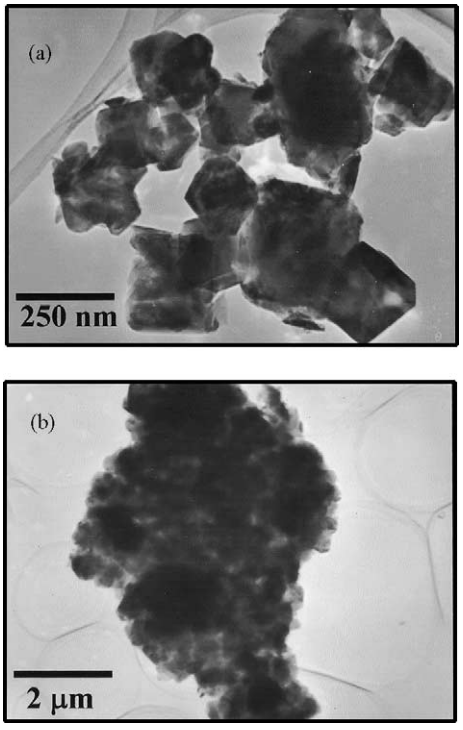

Fig. 3. TEM bright-field images of $LiMn_{0.5}Cr_{0.5}O_2$ calcined at 850 °C for (a) 12 h and (b) 24 h in an Ar atmosphere.

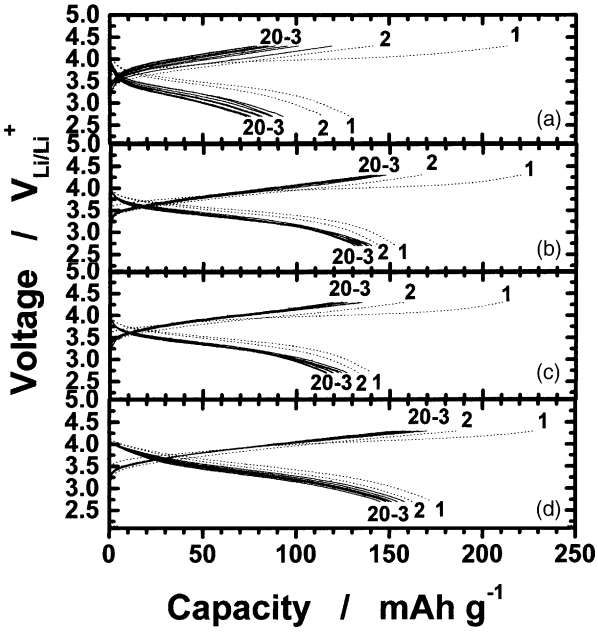

Fig. 4. Continuous charge–discharge curves of initial 20 cycles for $LiMn_{0.5}Cr_{0.5}O_2$ calcined at 850 °C for (a) 2 h, (b) 12 h, (c) 24 h, and (d) $LiMn_{0.6}Cr_{0.4}O_2$ calcined at 850 °C for 12 h in an Ar atmosphere. Dash line indicating 10 mA g^{-1} of current density and straight line meaning 20 mA g^{-1}.

to be 300 nm in diameter. In contrast, the calcined particles are highly agglomerated after 24 h of firing shown in Fig. 3b. These different particle morphologies may lead to different electrochemical properties. From the above results, it is concluded that a wide range of solid solution in $LiMn_x^{III}Cr_{1-x}^{III}O_2$ was achieved with the help of homogeneous emulsion, and this preparation route is potentially advantageous to synthesize oxide cathode material for Li-ion batteries.

3.2. Electrochemistry

The voltage profiles of $Li/LiMn_xCr_{1-x}O_2$ ($x = 0.5$ and 0.6) between 2.7 and 4.3 V versus Li are shown in Fig. 4. A current density of 10 mA g^{-1} was applied for the initial two cycles, and subsequently the cell was cycled with a current density of 20 mA g^{-1}. All samples showed similar initial charge capacities of about 220 mAh g^{-1}. This reaction is considered to be electrochemical oxidation of Mn and Cr [18], because the average oxidation state of both Mn and Cr are 3+, respectively, as verified by XANES in Fig. 2. Cr itself in $LiCrO_2$ shows a poor electrochemical activity in this potential range [18]. However, one interesting aspect of these kinds of compounds is that Cr in Mn doped $LiCrO_2$ can join in the electrochemical reaction. However, these materials exhibited a large irreversible capacity during the first cycle. Obviously, calcination for 12 h led to relatively higher reversible capacity due probably to the structural integrity and powder morphology. As expected from the TEM results in Fig. 3, well-dispersed powders exhibited somewhat higher capacity (Fig. 4b). From the second cycle, reversible Li^+ de-/intercalation reactions are observed. Considering the Mn substitution amount, the reversible capacity is enhanced by higher level Mn doping (Fig. 4d). This may be due to the higher *c*/*a* ratio as described in Table 2. Average operation voltage is also higher for higher levels of substitution, $LiMn_{0.6}Cr_{0.4}O_2$. A slow capacity loss on cycling was observed, which is due primarily to the irreversible redox of the $Cr^{3+/6+}$ couple according to our XANES results [27]. It is previously reported that layered orthorhombic and monoclinic $LiMnO_2$ oxides transform to spinel-like structure during cycling, showing two clear potential plateaus at 3 and 4 V versus Li. As can be seen in Fig. 4, there is no appearance of phase transformation upon cycling, because all charge and discharge curves show S-shape potential changes. From these results, it is concluded that the prepared $LiMn_xCr_{1-x}O_2$ compounds are electrochemically active with good reversibility. Details of electrochemical reaction mechanism are still under investigation and will be reported in near future.

4. Conclusion

In attempts to prepare a wide range of solid solutions, direct mixing by grinding the starting materials usually results in undesired impurity phases in the final product. In the present work, the drawback of the conventional method was significantly suppressed by employing the

emulsion drying method. The emulsion drying method gives a very homogeneous powder precursor so that it was possible to enlarge the solid solution range of $LiMn_xCr_{1-x}O_2$ ($0 \leq x \leq 0.6$). From the XANES study, it was found that the prepared powders consisted of trivalent Mn and Cr. The obtained capacity was improved by substituting more amount of Mn in $LiCrO_2$ structure.

Acknowledgements

The authors would like to thank N. Kumagai and Mr. K. Kurihara, Iwate University, for helpful assistance in the experimental work. This study was supported by NEDO of Japan, and Saneyoshi Scholarship Foundation. STM personally acknowledges Yoneyama Studentship.

References

[1] K. Mizushima, P.C. Jones, P.J. Wiseman, J.B. Goodenough, Mater. Res. Bull. 15 (1980) 783.
[2] B. Garcia, J. Farcy, J.P. Pereira-Ramos, J. Perichon, N. Baffier, J. Power Sources 54 (1995) 373.
[3] C. Delmas, I. Saadoune, Solid State Ionics 53–56 (1992) 370.
[4] R.J. Gummow, A. de Kock, M.M. Thackeray, Solid State Ionics 69 (1994) 59.
[5] T. Ohzuku, M. Kitagawa, T. Hirai, J. Electrochem. Soc. 137 (1990) 769.
[6] A.R. Amstrong, P.G. Bruce, Nature 381 (1996) 499.
[7] B. Ammundsen, J. Desilvestro, T. Groutso, D. Hassell, J.B. Metson, E. Regan, R. Steiner, P.J. Pickering, J. Electrochem. Soc. 147 (2000) 4078.
[8] Y.-I. Jang, B. Huang, H. Wang, D.R. Sadoway, Y.-M. Chiang, J. Electrochem. Soc. 146 (1999) 3217.
[9] L. Croguennec, P. Deniard, R. Brec, J. Electrochem. Soc. 144 (1997) 3323.
[10] S.-T. Myung, S. Komaba, N. Kumagai, K. Kurihara, Chem. Lett. (2001) 1114.
[11] S.-T. Myung, S. Komaba, N. Kumagai, Electrochim. Acta 47 (2002) 3287.
[12] S.-T. Myung, S. Komaba, N. Kumagai, J. Electrochem. Soc. 149 (2002) A1349.
[13] Y.-M. Chiang, H. Wang, Y.-I. Jang, Chem. Mater. 13 (2001) 53.
[14] J.R. Dahn, T. Zheng, C.L. Thomas, J. Electrochem. Soc. 145 (1998) 851.
[15] I.J. Davidson, R.S. Mcmillan, H. Slegr, B. Luan, I. Kargina, J.J. Murray, I.P. Swainson, J. Power Sources 81 (1999) 406.
[16] B. Ammundsen, J. Paulsen, I. Davidson, R.S. Liu, C.H. Shen, J. M Chen, L.Y. Jang, J.F. Lee, J. Electrochem. Soc. 149 (2002) A431.
[17] M. Balasubramanian, J. McBreen, I.J. Dadvison, P.S. Whitefield, I. Kargina, J. Electrochem. Soc. 149 (2002) A176.
[18] S.-T. Myung, S. Komaba, N. Hirosaki, N. Kumagai, Electrochem. Commun. 4 (2002) 397.
[19] S.-T. Myung, S. Komaba, N. Kumagai, J. Electrochem. Soc. 148 (2001) A482.
[20] S. Komaba, K. Oikawa, S.-T. Myung, N. Kumagai, T. Kamiyama, Solid State Ionics 149 (2002) 47.
[21] S.-T. Myung, S. Komaba, N. Kumagai, H. Yashiro, H.-T. Chung, T.-H. Cho, Electrochim. Acta 47 (2002) 2543.
[22] S.-T. Myung, H.-T. Chung, J. Power Sources 84 (1999) 32.
[23] S.-T. Myung, N. Kumagai, S. Komaba, H.-T. Chung, J. Appl. Electrochem. 30 (2000) 1081.
[24] T. Roisnel, J. Rodriguez-Carjaval, Fullprof Manual, Institut Laue-Langevin, Grenoble, 2000.
[25] S.K. Mishra, G. Ceder, Phys. Rev. B 59 (1999) 6120.
[26] H. Yamauchi, A. Yamada, H. Uwe, Phys. Rev. B 58 (1998) 8.
[27] S.-T. Myung, S. Komaba, N. Hirosaki, N. Kumagai, K. Arai, R. Kodama, I. Nakai, J. Electrochem. Soc., submitted for publication.